First-principles phonon calculations of thermal expansion in Ti_3SiC_2, Ti_3AlC_2, and Ti_3GeC_2

Atsushi Togo,[1,2,*] Laurent Chaput,[3] Isao Tanaka,[2,4] and Gilles Hug[1]
[1]*Laboratoire d'Etude des Microstructures, UMR 104, ONERA-CNRS ONERA, BP 72, 92322 Châtillon Cedex, France*
[2]*Department of Materials Science and Engineering, Kyoto University, Sakyo, Kyoto 606-8501, Japan*
[3]*CNRS–Institut des Sciences des Matériaux de Mulhouse, 4 rue des Frères Lumiere, 68093 Mulhouse, France*
[4]*Nanostructures Research Laboratory, Japan Fine Ceramics Center, Atsuta, Nagoya 456-8587, Japan*
(Received 30 January 2010; revised manuscript received 9 April 2010; published 4 May 2010)

Thermal properties of ternary carbides with composition Ti_3SiC_2, Ti_3AlC_2, and Ti_3GeC_2 were studied using the first-principles phonon calculations. The thermal expansions, the heat capacities at constant pressure, and the isothermal bulk moduli at finite temperatures were obtained under the quasiharmonic approximation. Comparisons were made with the available experimental data and excellent agreements were obtained. Phonon band structures and partial density of states were investigated. These compounds present unusual localized phonon states at low frequencies, which are due to atomiclike vibrations parallel to the basal plane of the Si, Al, or Ge elements.

DOI: 10.1103/PhysRevB.81.174301 PACS number(s): 63.20.dk, 65.40.De

I. INTRODUCTION

The isomorphic ternary carbides of Ti_3AC_2 (where A=Si, Al, and Ge) have attracted attention due to their unique combination of properties: good thermal and electrical conductivities, high elastic modulus, light weight, and thermal stabilities.[1–4] All those properties depend crucially on the phonon spectrum. Whereas the elastic properties are mainly determined by the small-wave-vector limit of the phonon frequencies, it is the full band structure which is relevant to understand the thermal conductivity.

The crystal structure of Ti_3AC_2 whose space group is $P6_3/mmc$ (No. 194) is shown in Fig. 1. It is composed of Ti, A, and C hexagonal layers as denoted on the right side of the crystal structure. The unit cell contains 12 atoms, where each one is located in a layer. However, the structure is described by only four independent Wyckoff positions. There are two different crystallographic sites for the Ti atoms and one for the A and C atoms. We define the Ti sites between the C layers as Ti-1 and those between the C and A layers as Ti-2. In between two adjacent A layers, three Ti layers are stacked in the same manner as the face-centered cubic. The C atoms occupy the octahedral cavities defined by the three Ti layers. Since every A layer is in a mirror plane, the stacking of the three Ti layers are flipped alternately, which makes this unit cell long along c axis.

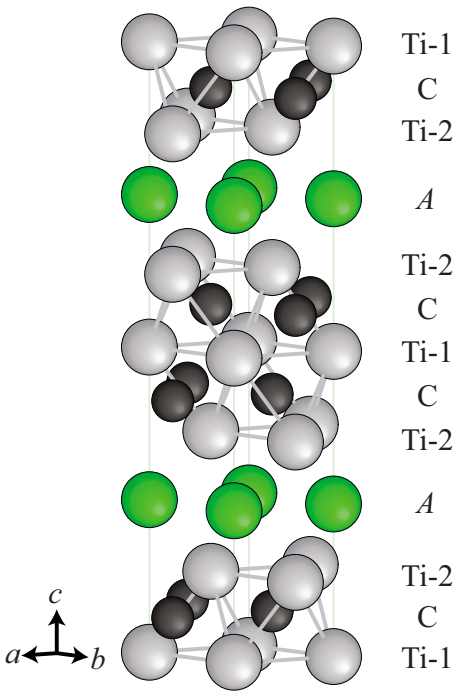

FIG. 1. (Color online) Crystal structure of Ti_3AC_2 ($P6_3/mmc$).

Barsoum *et al.* found from neutron diffraction that the Si atoms in Ti_3SiC_2 exhibit substantially higher vibration amplitudes than the other atoms.[1] They ascribed this fact to a low Ti-Si bond strength as compared to other atomic bonds. In addition, they noted that the vibration is isotropic although curiously not at all temperatures.

In this paper, thermal properties of Ti_3SiC_2, Ti_3AlC_2, and Ti_3GeC_2 at constant pressure were investigated using the first-principles phonon calculations. Thermal expansions, heat capacities, and isothermal bulk moduli are presented. Their characteristic phonon features are discussed using phonon band structures and partial density of states (PDOS).

II. METHOD OF CALCULATION

A. Thermal properties

The thermal properties of solids at constant volume can be calculated from their phonon density of states as a function of frequencies. The phonon contribution to the Helmholtz free energy F_{phonon} is given by

$$F_{\mathrm{phonon}} = \frac{1}{2}\sum_{\mathbf{q},\nu} \hbar\omega_{\mathbf{q},\nu} + k_{\mathrm{B}}T \sum_{\mathbf{q},\nu} \ln[1-\exp(-\hbar\omega_{\mathbf{q},\nu}/k_{\mathrm{B}}T)], \tag{1}$$

where $\mathbf{q}$ and ν are the wave vector and band index, respectively, $\omega_{\mathbf{q},\nu}$ is the phonon frequency at $\mathbf{q}$ and ν, and T is the

temperature. k_B and $\hbar$ are the Boltzmann constant and the reduced Planck constant, respectively. The heat capacity C_V and the entropy S at constant volume are given by

$$C_V = \sum_{\mathbf{q},\nu} k_B \left(\frac{\hbar\omega_{\mathbf{q},\nu}}{k_B T}\right)^2 \frac{\exp(\hbar\omega_{\mathbf{q},\nu}/k_B T)}{[\exp(\hbar\omega_{\mathbf{q},\nu}/k_B T)-1]^2} \quad (2)$$

and

$$S = -k_B \sum_{\mathbf{q},\nu} \ln[1-\exp(-\hbar\omega_{\mathbf{q},\nu}/k_B T)] - \frac{1}{T}\sum_{\mathbf{q},\nu} \frac{\hbar\omega_{\mathbf{q},\nu}}{\exp(\hbar\omega_{\mathbf{q},\nu}/k_B T)-1}, \quad (3)$$

respectively.

In practical thermodynamical problems related to solids, the thermal properties need to be known at constant pressure. They can be calculated from the previous quantities through thermodynamic relationship. The Gibbs free energy G may be written as

$$G(T,p) = \min_V [U(V) + F_{\text{phonon}}(T;V) + pV], \quad (4)$$

where V and p are the volume and pressure, respectively, and $U(V)$ is the total energy of electronic structure at constant volume. The right-hand side of Eq. (4) means that, for each couple of T and p variables, the function inside the square brackets is minimized with respect to the volume. Then the heat capacity at constant pressure is derived from $G(T,p)$ by

$$C_P(T,p) = -T\frac{\partial^2 G(T,p)}{\partial T^2} = T\frac{\partial V(T,p)}{\partial T}\frac{\partial S(T;V)}{\partial V}\bigg|_{V=V(T,p)} + C_V[T,V(T,p)], \quad (5)$$

where $V(T,p)$ is the equilibrium volume at T and p.

B. Computational details

In this work, we have employed the so-called quasiharmonic approximation (QHA) to calculate the thermal properties at constant pressure. $U(V)$ and $F_{\text{phonon}}(T;V)$ were calculated at 13 volume points, and the thermodynamic functions of the right-hand side of Eq. (4) were fitted to the integral form of the Vinet equation of state (EOS) (Ref. 5) at $p=0$. Gibbs free energies at finite temperatures were obtained as the minimum values of the thermodynamic functions, and the corresponding equilibrium volumes and isothermal bulk moduli were obtained simultaneously from the Vinet EOS. Unit cells used to calculate $U(V)$ and $F_{\text{phonon}}(T;V)$ were relaxed by the first-principles calculation under the hydrostatic-stress conditions. These procedures applied for Ti_3SiC_2 are demonstrated in Fig. 2, where $U(V)+F_{\text{phonon}}(T;V)$ as a function of unit-cell volume at temperatures are shown. The thermal expansion is observed as an increase in the equilibrium volume. For C_P, the right-hand side of Eq. (5) was calculated by numerical differentiation for $\partial V/\partial T$ and by polynomial fittings for S and C_V with respect to volume. S and C_V were well fitted by polynomial functions.

For the first-principles calculations, we employed the plane-wave basis projector augmented wave (PAW) method[6]

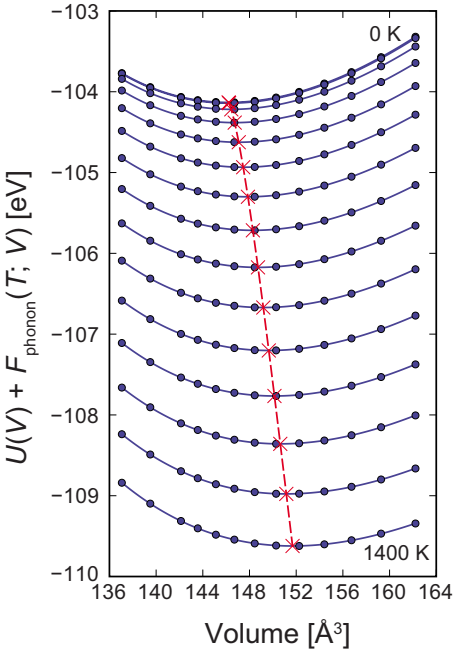

FIG. 2. (Color online) $U(V)+F_{\text{phonon}}(T;V)$ as a function of unit-cell volume of Ti_3SiC_2. The circles denote $U(V)+F_{\text{phonon}}(T;V)$ calculated at the volume points at every 100 K between 0 and 1400 K. The solid curves show the fitted thermodynamic functions. The minimum values of the fitted thermodynamic functions at temperatures are depicted by the crosses. The dashed curve passing through the crosses is guide to the eye.

in the framework of the density-functional theory within the generalized gradient approximation (GGA) in the Perdew-Burke-Ernzerhof form[7] as implemented in the VASP code.[8–10] A plane-wave energy cutoff of 500 eV was used. The radial cutoffs of the PAW potentials of Ti, Si, Al, Ge, and C were 1.32, 1.01, 1.01, 1.22, and 0.79 Å, respectively. The 3*p*, 3*d*, and 4*s* electrons for Ti, the 3*s* and 3*p* electrons for Si and Al, the 4*s* and 4*p* electrons for Ge, and the 2*s* and 2*p* electrons for C were treated as valence and the remaining electrons were kept frozen. The Brillouin zones of the unit cells were sampled by a $16\times16\times2$ *k*-point mesh, and the Methfessel-Paxton scheme[11] with a smearing width of 0.4 eV was employed.

Phonon calculations were performed by the supercell approach. Real-space force constants of supercells were calculated in the density-functional perturbation theory (DFPT) implemented in the VASP code,[12] and phonon frequencies were calculated from the force constants using the PHONOPY code.[13,14] For the QHA calculations, supercells containing $2\times2\times1$ unit cells were used. To evaluate supercell size dependency of phonon property, Helmholtz free energies were calculated with $1\times1\times1$, $2\times2\times1$, and $4\times4\times1$ supercells for the three compounds using the Parlinski-Li-Kawazoe method[15] with a finite displacement (FD) of 0.01 Å. In Table I, Helmholtz free energies with respect to supercell size and method of force-constant calculation at 300 and 1000 K are shown. The difference between the DFPT and FD method is negligible. The energy differences between supercell sizes increase with increasing temperature. Between $1\times1\times1$ and $4\times4\times1$ supercells, the energy differences at 1000 K are

TABLE I. Helmholtz free energies with respect to supercell size and method of force-constant calculation at 300 and 1000 K. The energies are given in eV/unit cell.

Supercell size	Ti_3SiC_2	Ti_3AlC_2	Ti_3GeC_2
	300 K		
$1\times1\times1$ (FD)	0.548	0.517	0.444
$2\times2\times1$ (DFPT)	0.615	0.590	0.527
$2\times2\times1$ (FD)	0.615	0.589	0.526
$4\times4\times1$ (FD)	0.609	0.592	0.522
	1000 K		
$1\times1\times1$ (FD)	2.324	2.418	−2.649
$2\times2\times1$ (DFPT)	−2.144	−2.218	−2.409
$2\times2\times1$ (FD)	−2.145	−2.219	−2.411
$4\times4\times1$ (FD)	−2.164	−2.208	−2.426

several hundreds of meV/unit cell, however those between $2\times2\times1$ and $4\times4\times1$ supercells reduce to several tens of meV/unit cell. We chose the $2\times2\times1$ supercells to calculate thermal properties; however it has to be taken into account that Grabowski *et al.*[16] reported that small error in phonon calculation may result in significant change in the calculated thermal properties, especially at high temperatures.

III. RESULTS AND DISCUSSION

A. Thermal expansion, heat capacity at constant pressure, and isothermal bulk modulus

Volume expansions of the three compounds as a function of temperature are shown in Fig. 3. Volume expansion is defined by $\Delta L/L_0$, where L_0 is $L=V^{1/3}$ at 300 K and $\Delta L=L-L_0$. The calculated values of Ti_3SiC_2 are in good agreement with the experimental values of Refs. 1 and 17. The experimental values of Ref. 18 are smaller than the others. The

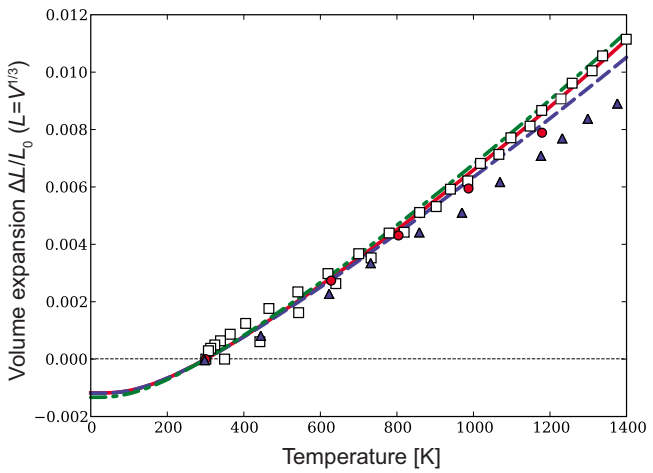

FIG. 3. (Color online) Volume expansions, $\Delta L/L_0$ ($L=V^{1/3}$), as a function of temperature. The solid, dashed, and dashed-dotted curves denote those of Ti_3SiC_2, Ti_3AlC_2, and Ti_3GeC_2, respectively. The experimental values of Ti_3SiC_2 are depicted by the circles (Ref. 1), squares (Ref. 17), and triangles (Ref. 18).

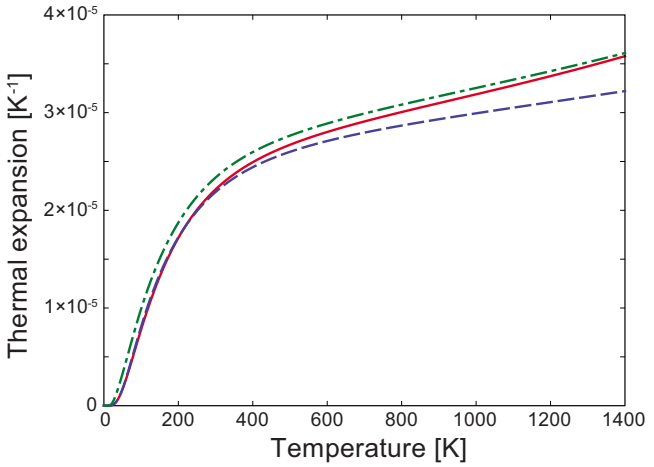

FIG. 4. (Color online) Thermal expansion coefficients as a function of temperature. The solid, dashed, and dashed-dotted curves denote those of Ti_3SiC_2, Ti_3AlC_2, and Ti_3GeC_2, respectively.

volumes were overestimated between 2.3% at 300 K and 2.5% at 1179 K in comparison to those in Ref. 1. This nearly constant overestimation is probably due to the tendency of the GGA and is hidden in the volume expansion since the volume expansion is a function of volume ratio. The volume expansions of the three compounds are found $Ti_3AlC_2 < Ti_3SiC_2 < Ti_3GeC_2$, however the differences among them are small.

The thermal expansion coefficients, $\frac{1}{V}\frac{\partial V}{\partial T}$, of the three compounds are shown in Fig. 4. With increasing temperature, the thermal expansion coefficients grow rapidly up to ~400 K, and the slopes become smaller and nearly constant at high temperatures. Below ~200 K, those of Ti_3SiC_2 and

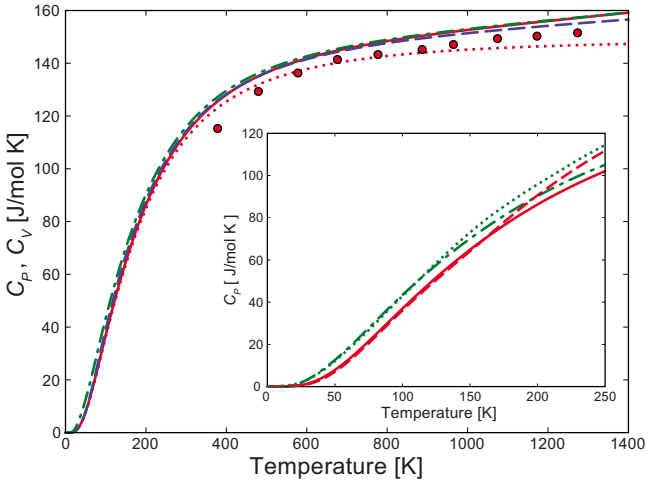

FIG. 5. (Color online) Heat capacities as a function of temperature. The solid, dashed, and dashed-dotted curves denote C_P of Ti_3SiC_2, Ti_3AlC_2, and Ti_3GeC_2, respectively. The circles depict the experimental values of C_P of Ti_3SiC_2 (Ref. 1). The dotted curve denotes C_V of Ti_3SiC_2. Inset is the magnified figure below 250 K for Ti_3SiC_2 and Ti_3GeC_2. The solid and dashed-dotted curves in the inset denote C_P of Ti_3SiC_2 and Ti_3GeC_2, respectively. The dashed and dotted curves in the inset show the experiments of Ti_3SiC_2 (Ref. 19) and Ti_3GeC_2 (Ref. 20), respectively.

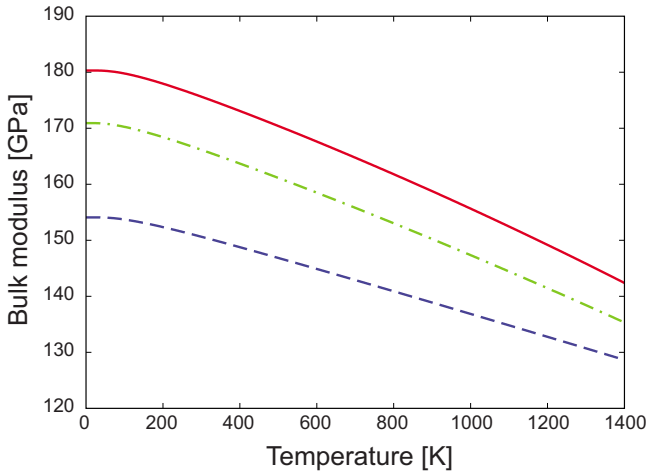

FIG. 6. (Color online) Isothermal bulk moduli as a function of temperature. The solid, dashed, and dashed-dotted curves denote those of Ti_3SiC_2, Ti_3AlC_2, and Ti_3GeC_2, respectively.

Ti_3AlC_2 are equivalent and are smaller than that of Ti_3GeC_2. At high temperatures, those of Ti_3SiC_2 and Ti_3GeC_2 are equivalent and are larger than that of Ti_3AlC_2.

The heat capacities C_P of the three compounds as a function of temperature are shown in Fig. 5. Below ~120 K, those of Ti_3SiC_2 and Ti_3GeC_2 agree well with respective experimental values reported by Drulis *et al.*[19,20] Above ~120 K, the experiments show larger C_P than the calculations. The values of Ti_3SiC_2 at high temperatures are in good agreement with the experimental values reported by Barsoum *et al.*[1] although the calculation slightly overestimates the experiment. The differences among the three compounds are small through the temperature range. At low temperatures, C_P of Ti_3SiC_2 and Ti_3AlC_2 are equivalent and are slightly smaller than that of Ti_3GeC_2. With increasing temperature, C_P of Ti_3GeC_2 approaches to that of Ti_3SiC_2, and that of Ti_3AlC_2 becomes smaller than that of Ti_3SiC_2. In Fig. 5, C_V of Ti_3SiC_2 with a fixed volume that was relaxed under the zero hydrostatic-stress condition is also shown. At low temperatures, C_V is equivalent to C_P. At high temperatures, C_P keeps positive slope as well as the experiment, however C_V saturates.

Isothermal bulk moduli as a function of temperature are shown in Fig. 6. Among the three compounds, through the temperature range, Ti_3SiC_2 and Ti_3AlC_2 have the highest and the lowest bulk moduli, respectively, i.e., Ti_3SiC_2 is the most incompressible and Ti_3AlC_2 is the most compressible. This trend agrees with the experiments: 190,[4] 185,[21] 187,[21] 179,[22] and 206 GPa (Ref. 23) for Ti_3SiC_2, 156 (Ref. 24) and 165 GPa (Ref. 21) for Ti_3AlC_2, 186 (Ref. 4) and 197 GPa (Ref. 25) for Ti_3GeC_2. With increasing temperature, the bulk moduli of the three compounds decrease and the differences among the bulk moduli become small.

B. Phonon band structure and partial density of states

The phonon band structures and PDOS of the three compounds, which were calculated using $4\times4\times1$ supercells, are shown in Figs. 7 and 8, respectively. These band structures have common framework. There is a band gap starting around 13 THz. Below this band gap, the acoustic modes disperse up to ~7 THz. The band structure along the path Γ-*M*-*K*-Γ is similar to that along the path *A*-*L*-*H*-*A*, which means, on average, the dispersion in the *z* direction is small. Therefore smaller interaction is expected in the *z* direction, and this implies that thermal conductivity is smaller in the *z* direction than in the basal plane. Some characteristic differences among the three compounds can be found at the low frequencies, where two flat bands for Ti_3SiC_2 and Ti_3AlC_2 and three flat bands for Ti_3GeC_2 are observed near the *M*-*K* and *L*-*H* band paths.

These flat bands, which correspond to the peaks in the phonon PDOS, indicate localization of the states, i.e., they behave like "atomic states." As shown in Fig. 8, the peaks at low frequencies are composed of states of *A* atoms and a small fraction of states of Ti-2 atoms. The peaks of Si and Al states and the two lower peaks of Ge states are composed of those atomic vibrations that are parallel to the basal plane (*A*-*xy*). The phonon frequencies of the lower two peaks of Ti_3GeC_2 are lower than those of the other compounds since atomic mass of Ge is heavier than those of Si and Al. The third peak from the bottom of the Ge states consists of the atomic vibrations perpendicular to the basal plane (Ge-*z*). By contrast, the Si-*z* and Al-*z* states are relatively delocalized.

Above the band gap, the density of states are mostly composed of C states since its atomic mass is much lighter than those of the other atoms. The C-*z* states are more localized than C-*xy* states since interlayer interaction is not likely to occur at high frequencies.

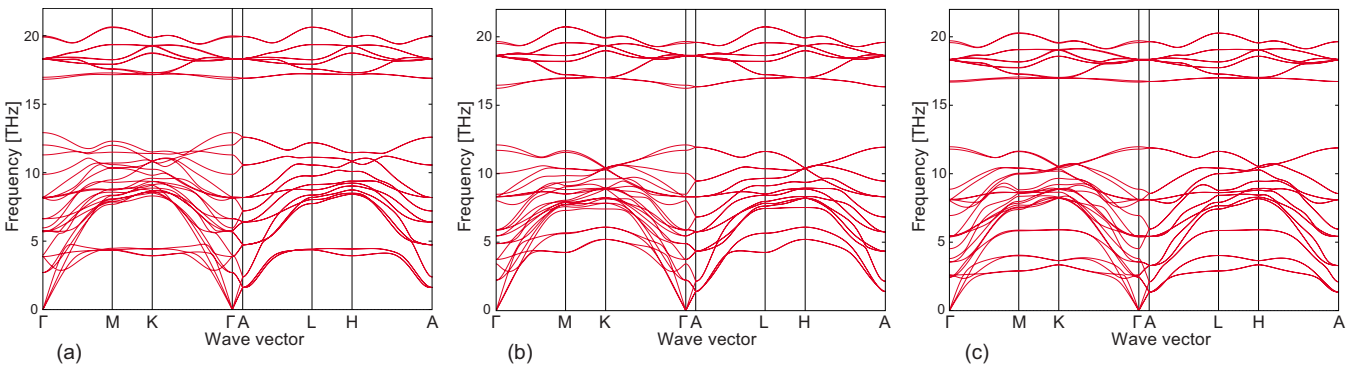

FIG. 7. (Color online) Phonon band structures of (a) Ti_3SiC_2, (b) Ti_3AlC_2, and (c) Ti_3GeC_2.

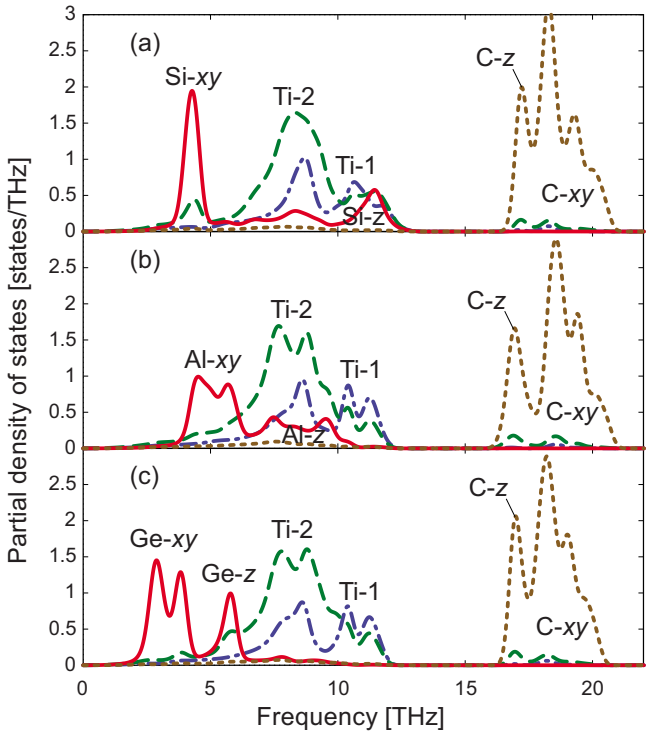

FIG. 8. (Color online) Phonon partial density of states of (a) Ti_3SiC_2, (b) Ti_3AlC_2, and (c) Ti_3GeC_2. The dashed-dotted, dashed, and dotted curves denote those of Ti-1, Ti-2, and C, respectively, and those of Si, Al, and Ge are depicted by the solid curves. The *xy* and *z* labels attached to the chemical symbols indicate that those atomic vibrations parallel to and perpendicular to the basal plane, respectively, are dominant.

The phonon-PDOS shapes of the Ti-1 and Ti-2 states of Ti_3AlC_2 and Ti_3GeC_2 are quite similar. Interestingly, the corresponding PDOS of Ti_3SiC_2 exhibit clear differences from the formers. For example, there is one main peak in the Ti-2 states of Ti_3SiC_2, whereas the corresponding peak is clearly split into two components in the other compounds. It is considered that the atomic radii of the Al and Ge atoms in these compounds are similar and any difference in the groups 13 and 14 of the periodic table that the *A* atom belongs to is irrelevant.

Barsoum *et al.* reported in their neutron-diffraction study that the Si atom vibrates anisotropically and with larger amplitude than the Ti and C atoms.[1] This is considered consistent with our results since the Si-*xy* states at lower frequencies gain more phonon population at finite temperatures than the other atomic modes. To understand *A*-*xy* states, we focus on the atomic motions at *K* and *M* points as representative points in the reciprocal space, since as shown in Fig. 7, the localization becomes stronger by getting away from the Γ point. At the *K* and *M* points, the atomic motions corresponding to the two lower localized bands are schematically shown in Fig. 9. These motions are nearly identical among the three compounds. The localized bands at the *K* point are doubly degenerate and one eigenvector components in the *xy* plane can be chosen to be proportional to $(1,i)$ on the *A* atoms. Thus the motions of the *A* atoms in these eigenmodes can be represented as rotations around their average positions

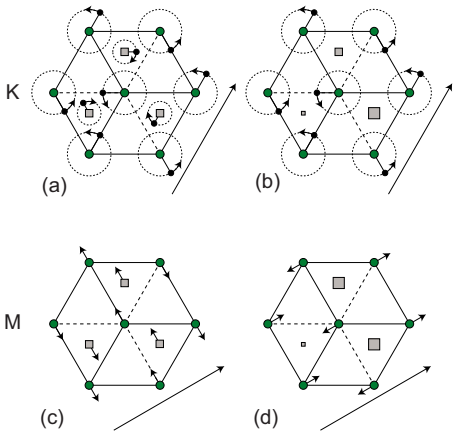

FIG. 9. (Color online) Atomic motions of the lower two localized bands at the *K* and *M* points. (a) and (b) are those at the *K* point, and (c) and (d) are those at the *M* point. The circle and square depict the *A* atom and Ti-2 atom, respectively. The size of square represents the position in the motion along *c* axis. It is shown larger when the Ti atoms displace closer to the *A* atom layer. Small arrows attached to the atoms show the directions of motions at a moment. The long arrows beside the hexagonal cells denote the directions of wave vectors.

as depicted in Figs. 9(a) and 9(b). At the *M* point, the phonon modes are approximately categorized as transverse waves [Fig. 9(c)] and longitudinal waves [Fig. 9(d)]. The atomic motions in these every phonon mode are well synchronized and correlated in order to avoid collisions between the *A* and Ti-2 atoms. The different shapes of the localized bands among the three compounds reflect the slight differences of interatomic interactions between the *A* and Ti-2 atoms.

IV. CONCLUSIONS

We studied the thermal properties of Ti_3SiC_2, Ti_3AlC_2, and Ti_3GeC_2 at constant pressure as a function of temperature using the first-principles phonon calculations. In the volume expansion and heat capacity, the differences among the three compounds are small. The volume expansion of Ti_3SiC_2 and the heat capacities of Ti_3SiC_2 and Ti_3GeC_2 agree well with the experiments. Through the calculated temperature range, Ti_3SiC_2 is the most incompressible and Ti_3AlC_2 is the most compressible. The differences of the isothermal bulk moduli among the three compounds decrease with increasing temperature. The phonon states were investigated using the phonon band structures and PDOS. It was demonstrated that the characteristic phonon band structure at low frequencies is related to localized Si, Al, or Ge atomic-vibrational states parallel to the basal plane.

ACKNOWLEDGMENTS

The French Agence Nationale de la Recherche (ANR) is acknowledged for financial support under Contract No. 07-MAPR-0015-04, and this work was also supported by Grants-in-Aid for Scientific Research (A), Scientific Research on Priority Areas (Grant No. 474), and the Global COE Program, all from MEXT, Japan.

*togo.atsushi@gmail.com

[1] M. W. Barsoum, T. El-Raghy, C. J. Rawn, W. D. Porter, H. Wang, E. A. Payzant, and C. R. Hubbard, J. Phys. Chem. Solids **60**, 429 (1999).
[2] M. W. Barsoum, Prog. Solid State Chem. **28**, 201 (2000).
[3] P. Finkel, M. W. Barsoum, J. D. Hettinger, S. E. Lofland, and H. I. Yoo, Phys. Rev. B **67**, 235108 (2003).
[4] P. Finkel *et al.*, Phys. Rev. B **70**, 085104 (2004).
[5] P. Vinet, J. H. Rose, J. Ferrante, and J. R. Smith, J. Phys.: Condens. Matter **1**, 1941 (1989).
[6] P. E. Blöchl, Phys. Rev. B **50**, 17953 (1994).
[7] J. P. Perdew, K. Burke, and M. Ernzerhof, Phys. Rev. Lett. **77**, 3865 (1996).
[8] G. Kresse, J. Non-Cryst. Solids **192-193**, 222 (1995).
[9] G. Kresse and J. Furthmüller, Comput. Mater. Sci. **6**, 15 (1996).
[10] G. Kresse and D. Joubert, Phys. Rev. B **59**, 1758 (1999).
[11] M. Methfessel and A. T. Paxton, Phys. Rev. B **40**, 3616 (1989).
[12] G. Kresse, M. Marsman, and J. Furthmüller, VASP the guide, http://cms.mpi.univie.ac.at/vasp/
[13] A. Togo, F. Oba, and I. Tanaka, Phys. Rev. B **78**, 134106 (2008).
[14] A. Togo, Phonopy, http://phonopy.sourceforge.net/
[15] K. Parlinski, Z. Q. Li, and Y. Kawazoe, Phys. Rev. Lett. **78**, 4063 (1997).
[16] B. Grabowski, L. Ismer, T. Hickel, and J. Neugebauer, Phys. Rev. B **79**, 134106 (2009).
[17] T. H. Scabarozi *et al.*, J. Appl. Phys. **105**, 013543 (2009).
[18] B. Manoun, S. K. Saxena, H. P. Liermann, and M. W. Barsoum, J. Am. Ceram. Soc. **88**, 3489 (2005).
[19] M. K. Drulis, A. Czopnik, H. Drulis, and M. W. Barsoum, J. Appl. Phys. **95**, 128 (2004).
[20] M. K. Drulis, A. Czopnik, H. Drulis, J. E. Spanier, A. Ganguly, and M. W. Barsoum, Mater. Sci. Eng., B **119**, 159 (2005).
[21] P. Finkel, M. W. Barsoum, and T. El-Raghy, J. Appl. Phys. **87**, 1701 (2000).
[22] P. Finkel, M. W. Barsoum, and T. El-Raghy, J. Appl. Phys. **85**, 7123 (1999).
[23] A. Onodera, H. Hirano, T. Yuasa, N. F. Gao, and Y. Miyamoto, Appl. Phys. Lett. **74**, 3782 (1999).
[24] H. B. Zhang, X. Wu, K. G. Nickel, J. X. Chen, and V. Presser, J. Appl. Phys. **106**, 013519 (2009).
[25] B. Manoun, H. Yang, S. K. Saxena, A. Ganguly, M. W. Barsoum, B. El Bali, Z. X. Liu, and M. Lachkar, J. Alloys Compd. **433**, 265 (2007).